Uptake of Gas-Phase Species by 1-Octanol. 2. Uptake of Hydrogen Halides and Acetic Acid as a Function of Relative Humidity and Temperature

H. Z. Zhang, Y. Q. Li,† and P. Davidovits*

Chemistry Department, Merkert Chemistry Center, Boston College, Chestnut Hill, Massachusetts 02467-3809

L. R. Williams, J. T. Jayne, C. E. Kolb, and D. R. Worsnop

Center for Aerosol and Cloud Chemistry, Aerodyne Research Inc., 45 Manning Road, Billerica, Massachusetts 01821-3976

Received: January 30, 2003; In Final Form: May 26, 2003

With use of a droplet train apparatus, the mass accommodation coefficients (α) of gas-phase HCl, HBr, HI, and CH_3COOH were measured for 1-octanol to probe the nature of the hydrophobic organic surface as a function of relative humidity and temperature (263−283 K). In the absence of water vapor, α for both HBr(g) and HI(g) is unity, independent of temperature. The mass accommodation coefficients for acetic acid and HCl are smaller, about 0.3 for acetic acid and 0.01 for HCl at 273 K, displaying negative temperature dependence. The value of α for acetic acid is independent of relative humidity. However, values of α for HBr, HI, and HCl change dramatically as a function of relative humidity. As the relative humidity increases, the α values for HBr and HI decrease, and α for HCl increases. At a relative humidity of about 50%, α for all three species converges to that on pure water. A model is proposed to explain these unexpected results.

Introduction

The importance of organic aerosols in tropospheric chemistry has been discussed in the Introduction to the preceding companion article[1] where we described uptake studies, using the droplet train apparatus, of several organic gas-phase species by 1-octanol, selected as a surrogate for hydrophobic oxygenated organic compounds. Here we present the second part of our octanol studies describing the uptake of gas-phase hydrogen halides (HI, HBr, HCl) and acetic acid (CH_3COOH) as a function of relative humidity and temperature. These studies yielded the mass accommodation coefficients of these species on octanol as a function of relative humidity and temperature. These studies revealed unexpected, interesting information about the nature of the octanol surface as a function of relative humidity.

Background technical information, description of the apparatus, basic experimental procedures, and data analysis used in this study are provided in the preceding companion article. Therefore, here, these aspects of the experiment will be presented only in brief outline.

Modeling Gas−Liquid Interactions

In our droplet train experiments, a gas-phase species (in this case the gas-phase acids) interacts with liquid droplets and the disappearance of that species from the gas phase is monitored. The disappearance of the species is expressed in terms of a measured uptake coefficient, γ_{meas}, which is related to the experimentally observed flux (J) into a surface via gas-phase density of the species (n_g) and the thermal mean speed ($\bar{c}$) as

$$J = \frac{n_g \bar{c} \gamma_{meas}}{4} \tag{1}$$

As is discussed in the companion paper, gas uptake is a function of several interrelated processes which may include gas-phase and liquid-phase diffusion, mass accommodation, Henry's law solubility, bulk phase, and surface reactivity. Therefore, the parameter γ_{meas} represents a convolution of these processes, and the experimental challenge is to separate the contributions of these processes to the overall gas uptake so as to obtain the value of the parameter of interest. Following the discussion in the previous paper and references therein, the overall uptake process is expressed in terms of a resistance formulation as

$$\frac{1}{\gamma_{meas}} = \frac{1}{\Gamma_{diff}} + \frac{1}{\gamma_0} \tag{2}$$

Here the parameter Γ_{diff} takes into account the effect of gas-phase diffusion on the uptake, and γ_0 is the uptake coefficient in the limit of "zero pressure", i.e., in the absence of gas-phase diffusion limitation. A modified Fuchs−Sutugin formulation for Γ_{diff} takes into account appropriately the effect of gas-phase diffusion on the uptake as

$$\frac{1}{\Gamma_{diff}} = \frac{0.75 + 0.283\mathrm{Kn}}{\mathrm{Kn}(1 + \mathrm{Kn})} \tag{3}$$

Here, Kn is the Knudsen number defined as $2\lambda/d_f$, where λ is the gas-phase mean free path. The mean free path is here expressed as $\lambda = 3D_g/\bar{c}$, where D_g is the gas-phase diffusion coefficient of the species. In the formulation of eq 3, $d_f = (2.0 \pm 0.1)d_o$, where d_o is the diameter of the droplet-forming orifice.[2]

The parameter γ_0 accounts for the effects on the gas uptake of the mass accommodation coefficient, Henry's law solubility, and liquid and surface reactions, if any. Because of solubility limitations, γ_{meas} is, in general, a function of the gas−liquid interaction time.

† Current address: Atmospheric Sciences Research Center, State University of New York, 251 Fuller Road, Albany, NY 12203.

10.1021/jp034254t CCC: $25.00
Published on Web 07/29/2003

A simple approximate expression for γ_0 is obtained by decoupling from each other the effects of mass accommodation and solubility. In such a simplified representation, the uptake coefficient Γ_{sat} takes into account the effect on the uptake of Henry's law solubility. In the absence of chemical reactions of the gas-phase species, γ_0 can be expressed as

$$\frac{1}{\gamma_0} = \frac{1}{\alpha} + \frac{1}{\Gamma_{sat}} \tag{4}$$

The parameter Γ_{sat} is given by eq 3 (see the note in ref 39 of the companion paper)

$$\frac{1}{\Gamma_{sat}} = \frac{\bar{c}}{8RTH}\sqrt{\frac{\pi t}{D_l}} \tag{5}$$

Here D_l is the liquid-phase diffusion coefficient of the species in octanol, t is the gas−liquid interaction time, R is the gas constant (L atm K^{-1} mol^{-1}), T is temperature, and H (M atm^{-1}) is the Henry's law constant. Note that Γ_{sat} measures the extent to which the gas-phase species is out of equilibrium with the liquid. As equilibrium is approached, Γ_{sat} approaches 0.

In a following section the mass accommodation process will be further examined to account for the uptake of gas-phase acids on octanol as a function of relative humidity.

Experimental Section

Uptake measurements in this study were performed by using the droplet train apparatus shown in Figure 1 of the preceding article. Briefly, in this apparatus gas uptake is measured by passing a fast-moving (1500−2800 cm/s) and monodisperse (150−300 μm in diameter) collimated train of octanol droplets through a 30 cm long, 1.4 cm diameter longitudinal low-pressure flow tube that contained trace amounts ($\sim 10^{13}$ to 10^{14} cm^{-3}) of the gases studied entrained in a flowing mixture of He carrier gas.

The carrier gases are introduced at the entrance of the reactor. The trace gases (diluted in He) are introduced through one of three loop injectors located along the flow tube. By selecting the injector and the droplet velocity, the gas−droplet interaction time can be varied between 2 and 15 ms.

The droplets are formed by forcing liquid octanol through a vibrating orifice located in a separate chamber. The liquid 1-octanol delivery lines were cooled to the desired droplet temperature. A chromel−alumel thermocouple in a stainless steel sheath was fixed in place just above the aperture and provided a continuous measure of the droplet stream temperature. The temperature of the droplets in the reaction zone is maintained by matching the partial pressure of the equilibrium 1-octanol vapor in this region. To study the effect of relative humidity on gas uptake, water vapor was added to the carrier gas flow. The equilibrium conditions governing octanol−water solutions are discussed in the preceding article.[1]

Gas uptake is determined by measuring the trace gas concentration (n_g) downstream of the flow tube as the surface area of the droplets is changed in a stepwise fashion, by varying the driving frequency of the piezoelectric ceramic. A measured decrease in the trace gas signal ($n_g - n_g'$) resulting from an increase in the exposed droplet surface area corresponds to an uptake of the gas by the droplet surface. The uptake coefficient (γ_{meas}), as defined in Zhang et al.,[1] was obtained from the measured change in trace gas signal via eq 6, where F_g is the carrier-gas volume rate of flow (cm^3 s^{-1}) through the system, $\Delta A = A_1 - A_2$ is the change in the total droplet surface area in contact with the trace gas, and n_g and n_g' are the trace gas densities at the outlet of the flow tube after exposure to droplets of area A_2 and A_1, respectively. Pressure balance in the system is monitored as discussed in Zhang et al.[1]

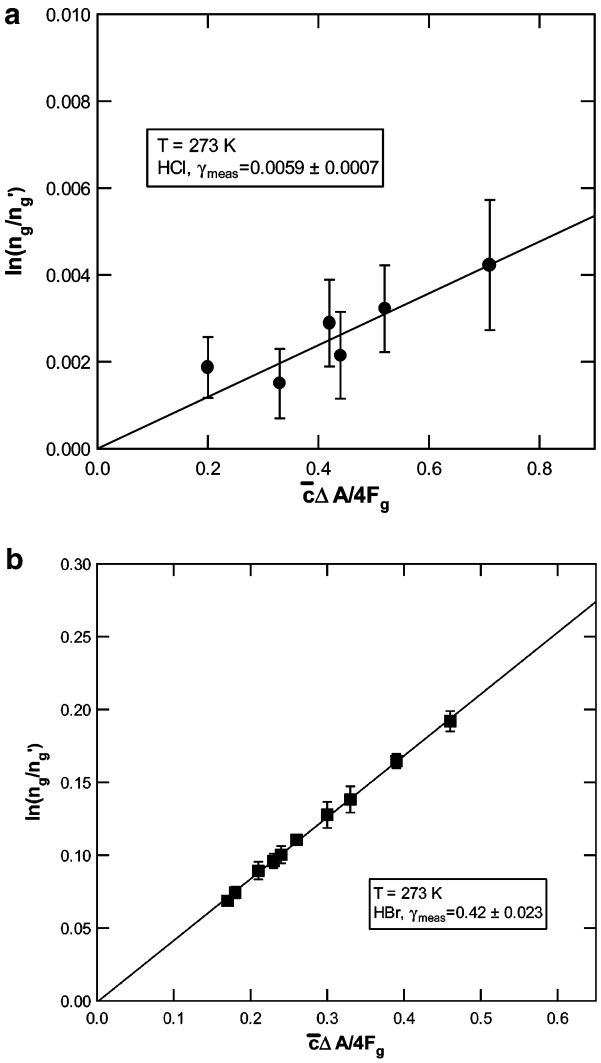

Figure 1. Experimental data showing plots of $\ln(n_g/n_g')$ as a function of $\bar{c}\Delta A/4F_g$ (a) for HCl and (b) for HBr, at droplet temperature T_d = 273 K. Solid lines are the least-squares fit to the data. The slope of the lines is γ_{meas}. Terms are defined in the text.

$$\gamma_{meas} = \frac{4F_g}{\bar{c}\Delta A}\ln\frac{n_g}{n_g'} \tag{6}$$

The gases HCl, HBr, and HI were obtained from Matheson Gas Products Inc. at >98% purity. The mass spectrum of normal acetic acid overlaps that of octanol. Therefore, to study the uptake of this molecule we used the 1-^{13}C isotope of acetic acid obtained from Cambridge Isotope Laboratories Inc. at 99% purity.

Results and Analysis

In panels a and b in Figure 1 we show plots of $\ln(n_g/n_g')$ at R.H. $\sim$ 0 for HCl and HBr as a function of $\bar{c}\Delta A/4F_g$ at 273 K. Here $\bar{c}\Delta A/4F_g$ was varied by changing the gas flow rate and the droplet surface area (ΔA). Due to solubility constraint, gas uptake under the stated conditions is a function of gas−liquid interaction time (t). The measurements shown in Figure 1a,b were obtained at t = 2.8 ms. Each point is the average of at

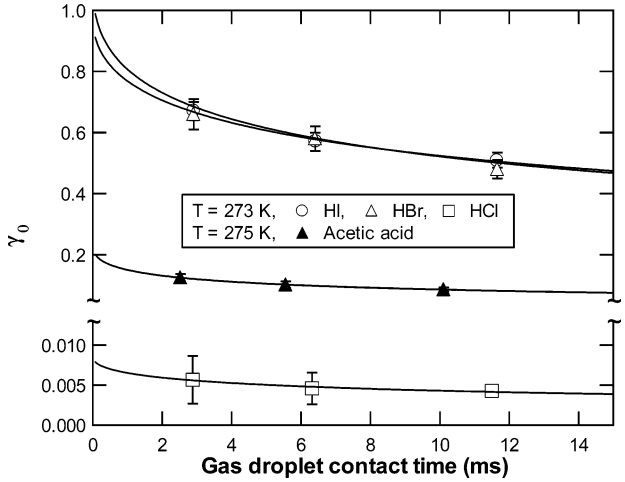

Figure 2. Uptake coefficient γ_0 as a function of gas-droplet contact time at R.H. = 0, for HCl (□), HBr (Δ), and HI (○) at droplet temperature $T_d = 273$ K and for acetic acid (▲) at $T_d = 275$ K. The solid line is the best fit to the data via eq 4 with Γ_{sat} given by eq 5.

TABLE 1: Gas-Phase Diffusion Coefficients, D_g (atm cm^2 s^{-1}), $T = 298$ K

	carrier gas	
trace gas	He	H_2O
HCl	0.701	0.166
HBr	0.610	0.130
HI	0.520	0.111
acetic acid	0.433	0.096

least 10 area change cycles and the error bars represent one standard deviation from the mean in the experimental $\ln(n_g/n_g')$ value. As is evident in eq 6, the slope of the plots in Figure 1a,b yields the value of γ_{meas}, with precision indicated in the following data: $\gamma_{meas} = 0.0059 \pm 0.0007$ and 0.42 ± 0.02 for HCl and HBr, respectively. Similar plots were obtained for a wide range of experimental parameters, for which the uptake fraction, $(n_g - n_g')/n_g$, varied from 5% to 50%. As is evident, in the absence of water vapor, γ_{meas} for HCl is almost 2 orders of magnitude smaller than γ_{meas} for HBr. Measurements of HI(g) and acetic acid uptake were conducted in the same way.

The effect of gas-phase diffusion on the uptake is taken into account by Γ_{diff} calculated from eq 3. The gas-phase diffusion coefficients (D_g) of HCl and acetic acid were taken from refs 4 and 5, respectively. These gas-phase diffusion coefficients vary as $T^{1.7}$ (helium as carrier gas) and $T^{2.0}$ (H_2O as carrier gas).[4] The D_g values for HBr and HI are calculated by using the method described by Reid et al.[6] The D_g values for 298 K are tabulated in Table 1. The parameter γ_0 is then obtained via eq 2.

In Figure 2, values of γ_0 on pure octanol are plotted as a function of gas−droplet contact time for HCl, HBr, and HI at 273 K and for acetic acid at 275 K. Note that the abscissa is broken so that we may display the much smaller γ_0 value for HCl in the same figure. The uptake for HBr, HI, and acetic acid is clearly time dependent, as is characteristic of solubility limited uptake. The time dependence of HCl uptake is less pronounced. The time dependence of γ_0 is expected to be given by the parameter Γ_{sat}. The solid lines in Figure 2 are plots of eq 4 with Γ_{sat} calculated from eq 5. As was stated in the preceding article, the coefficients H and D_l for octanol in eq 5 have not been measured, therefore, the product $H(D_l)^{1/2}$ was a variable in the fitting of the experimental points. In accord with eq 4, γ_0 at $t = 0$ is the mass accommodation coefficient α.

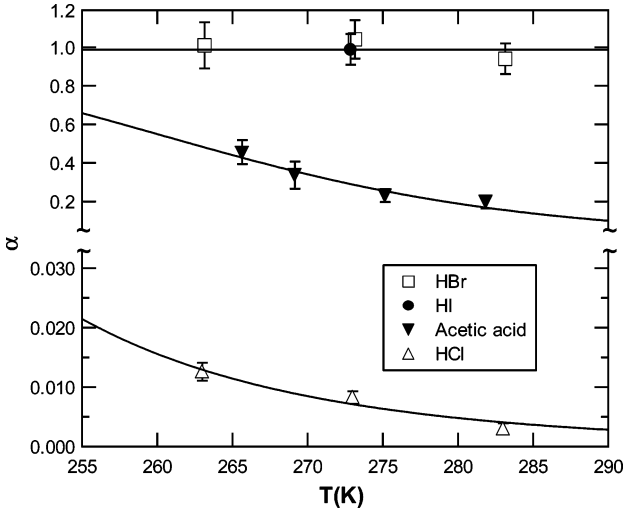

Figure 3. Mass accommodation coefficients (α) for HCl (Δ), HBr (□), HI (○), and acetic acid (▼) on 1-octanol as a function of temperature at R.H. = 0. The solid lines are best fit via eq 8.

Time dependent uptake studies were performed at three temperatures. The mass accommodation coefficients as a function of temperature for HCl, HBr, and acetic acid on octanol are shown in Figure 3. The mass accommodation coefficient for HI was measured only at 273 K. That point is also shown in the figure. Here again, the abscissa is broken to display α for all the species in the same figure. As is shown in Figure 3, within experimental accuracy, the mass accommodation coefficients for HBr(g) and HI(g) on pure octanol are unity, and for HBr, the mass accommodation coefficient is shown to be independent of temperature. The mass accommodation coefficient for HCl(g) on pure octanol exhibits negative temperature dependence and is about 2 orders of magnitude smaller than α for HBr and HI. The mass accommodation coefficient for acetic acid has likewise a negative temperature dependence. The magnitude of α for acetic acid ranges from about 0.2 at 283 K to 0.45 at 265 K.

To study the effect of water vapor on the uptake of gas-phase acids by octanol, we performed uptake studies at several water vapor pressures (relative humidity, R.H., ranging from ∼0 to 120%) as a function of droplet temperature and gas droplet contact time. The uptake coefficients γ_0 as a function of gas−droplet contact time for HCl, HBr, and HI at 273 K and for acetic acid at 266 K are shown in panels a, b, c, and d in Figure 4, respectively. For HCl and HBr, similar plots were also obtained at 263 and 283 K. The ^{13}C-labeled acetic acid is expensive. Therefore, the relative humidity studies for this species were done only at one temperature, 266 K. The solid lines in the figures are best fits of eq 4 to the experimental measurements, with Γ_{sat} given by eq 5, as outlined below. As before, γ_0 at $t = 0$ is the mass accommodation coefficient α.

The following features in the data shown in panels a−d in Figure 4 are immediately evident. The uptake of HCl increases with water vapor pressure while the uptake of HBr and HI decreases. Within experimental accuracy, the uptake of acetic acid is independent of relative humidity.

Further, data in Figure 4a−c show that with increasing water vapor pressure, the time dependence of the HCl uptake increases and the time dependence of the HBr and HI uptake decrease. This observation is explained in terms of the relative magnitudes of the parameters α and Γ_{sat} in eq 4. The larger the value of α the more pronounced is the effect on γ_0 of the time dependent term Γ_{sat}. The time dependence observed in Figure 4a−c follows

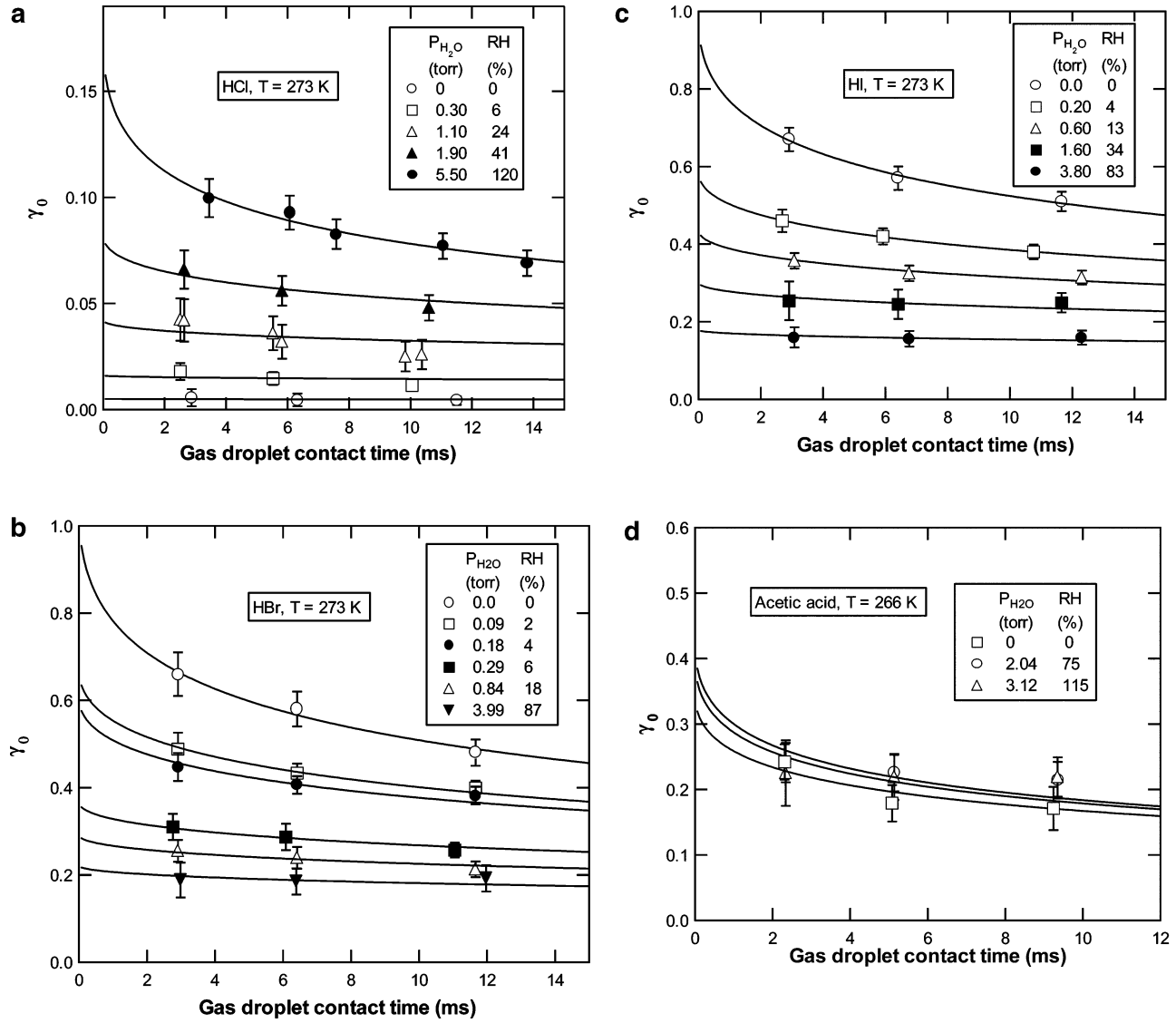

Figure 4. Uptake coefficient γ_0 as a function of gas−liquid contact time at different relative humidity (R.H.) values (a) for HCl at droplet temperature $T_d = 273$ K, R.H. = 0% (○), 6% (□), 24% (Δ), 41% (▲), 120% (●), (b) for HBr at $T_d = 273$ K, R.H. = 0% (○), 2% (□), 4% (●), 6% (■), 18% (Δ), 87% (▼); (c) for HI at $T_d = 273$ K, R.H. = 0% (○), 4% (□), 13% (Δ), 34% (■), 83% (●); and (d) for acetic acid at $T_d = 266$ K, R.H. = 0% (□), 75% (○), 115% (Δ). The solid line is the best fit to the data via eq 4 with Γ_{sat} given by eq 5.

because, as a function of relative humidity, Γ_{sat} remains constant, while α increases for HCl and decreases for HBr and HI.

Henry's Law Coefficients. As was previously stated, the coefficients H and D_l to be used in eq 5 have not been measured for octanol, therefore, the product $H(D_l)^{1/2}$ is a variable in the fitting of the experimental data shown in Figure 4a−d. In the preceding article,[1] we pointed to evidence that the Henry's law coefficient H and the diffusion coefficient D_l are not likely to be altered significantly by the water content of octanol at levels present in our experiments (<0.2 mol fraction). Therefore, in fitting of the time dependent uptake data for HCl, HBr, and acetic acid at a given temperature, the product $H(D_l)^{1/2}$ was held constant, independent of R.H. The $H(D_l)^{1/2}$ values are obtained from the best fits to the time dependent γ_0.

As pointed out in Appendix 2 of the preceding article,[1] the diffusion coefficients D_l in octanol can be calculated from the Hayduk−Minhas correlation.[6] With use of the calculated values for D_l, the Henry's law coefficients H were computed from the measured values of $HD_l^{1/2}$. These values of $HD_l^{1/2}$, D_l, and H are listed in Table 2. A best fit to the H values for HCl, HBr, and acetic acid in Table 2 yields the following expressions for

TABLE 2: Values of $HD_l^{1/2}$, D_l, and H for HCl, HBr, and Acetic Acid as a Function of Temperature

trace gas	T (K)	$HD_l^{1/2}$ (M cm atm^{-1} s$^{-1/2}$)	D_l (10^{-7}, cm^2 s^{-1})	H (10^3, M atm^{-1})
HCl	263	7.80 ± 0.50	7.98	8.73 ± 2.37
	273	6.10 ± 0.60	13.1	5.33 ± 1.67
	283	5.10 ± 1.89	20.8	3.54 ± 2.26
HBr	263	42.6 ± 8.02	7.28	49.9 ± 20.9
	273	28.6 ± 4.10	11.9	26.2 ± 9.61
	283	13.6 ± 1.80	18.8	9.92 ± 3.51
acetic acid	266	11.0 ± 2.30	5.14	15.3 ± 4.78
	275	4.04 ± 1.20	8.12	4.48 ± 1.82
	283	2.18 ± 1.00	11.0	2.08 ± 1.21

H. For HCl

$$\ln H\,(\mathrm{M/atm}) = -(5.87 \pm 1.46) + (3.96 \pm 0.39) \times 10^3/T \quad (7a)$$

For HBr

$$\ln H\,(\mathrm{M/atm}) = -(9.35 \pm 2.81) + (5.31 \pm 0.75) \times 10^3/T \quad (7b)$$

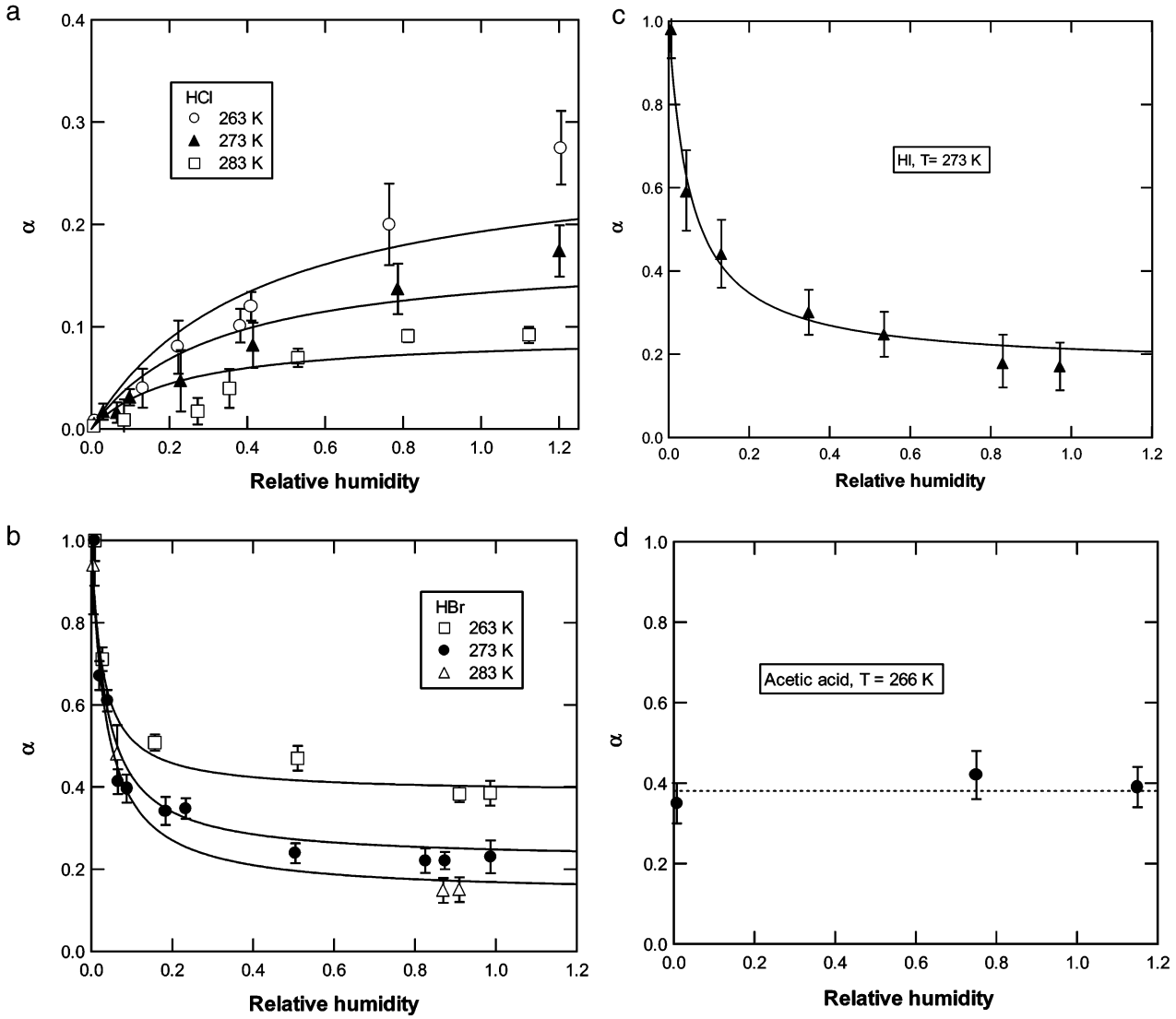

Figure 5. Mass accommodation coefficients (α) as a function of relative humidity (R.H.) at different temperatures: (a) HCl at 263 (○), 273 (▲), 283 K (□); (b) HBr at 263 (□), 273 (●), 283 K (Δ); (c) HI at 273 K (▲); and (d) acetic acid at 266 K (●). The solid lines are best fit via eq 16. Terms are defined in the text.

For acetic acid

$$\ln H\,(\mathrm{M/atm}) = -(30.3 \pm 6.90) + (10.6 \pm 1.85) \times 10^3/T \quad (7c)$$

Mass Accommodation Coefficient. The mass accommodation coefficients (α) for HCl, HBr, HI, and acetic acid as a function of relative humidity at the temperatures studied are shown in Figure 5, panels a, b, c, and d, respectively. The water vapor pressure at R.H. = 1 at 263, 273, and 283 K is 2.15, 4.58, and 9.21 Torr, respectively. The solid lines are the results of modeling via global fit of the experimental data at all the temperatures studied. To highlight the main features of the data, the mass accommodation coefficients as a function of water vapor pressure and relative humidity for HCl, HBr, and HI at 273 K and for acetic acid at 266 K are brought together in Figure 6.

Clearly, water vapor has a dramatic effect on the mass accommodation coefficient for the hydrogen halide gases. With increasing water vapor pressure, the magnitude of α decreases for HBr and HI and increases for HCl. At a relative humidity of about 50%, α for all three species converges to α on pure water and is about the same for all three species. This is evident from the listings in Table 3 that show α for HI, HBr, and HCl at 273 K on pure octanol, on octanol with about 100% R.H., and on pure water. The dramatic change in α with relative humidity for the hydrogen halides requires a deeper examination of the uptake process.

Discussion

Mass Accommodation on Pure Octanol. As is shown in Figure 3, within experimental accuracy, the mass accommodation coefficients for HBr(g) and HI(g) on pure octanol are unity, and for HBr, α is shown to be independent of temperature. (The mass accommodation coefficient for HI on pure octanol was measured at one temperature only.) The mass accommodation coefficient for HCl(g) on pure octanol exhibits negative temperature dependence and is about 2 orders of magnitude smaller than α for HBr and HI. The mass accommodation coefficient for acetic acid has likewise a negative temperature dependence with the magnitude of α ranging from about 0.2 at 280 K to 0.45 at 265 K.

In the preceding article we described mass accommodation as a two-step process involving surface adsorption followed by a competition between desorption from the surface (rate constant

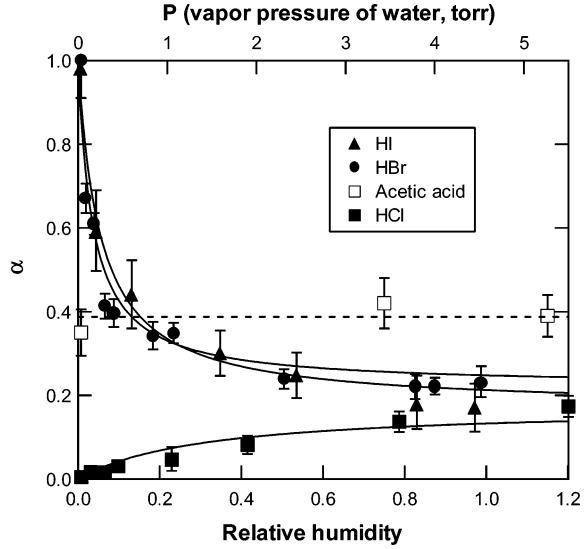

Figure 6. Mass accommodation coefficients (α) as a function of relative humidity (R.H.): HCl at 273 K (■); HBr at 273 K (●); HI at 273 K (▲); and acetic acid at 266 K (□). The solid lines are best fit via eq 16.

TABLE 3: Mass Accommodation Coefficients (α) for HCl, HBr, and HI at 273 K on Pure Octanol, on Octanol at 100% R.H., and on Pure Water

	α		
	on 1-octanol	on 1-octanol ~ 100% R.H.	on water
HCl	0.008 ± 0.001	0.17 ± 0.03	0.22 ± 0.03[a]
HBr	1.01 ± 0.11	0.21 ± 0.02	0.21 ± 0.03[b]
HI	0.98 ± 0.10	0.18 ± 0.05	0.17 ± 0.02[b]

[a] Van Doren et al.[24] [b] Zhang.[25]

k_{des}) and solvation into the bulk liquid (rate constant k_{sol}).[7−9] With the thermal accommodation equal to 1, the mass accommodation coefficient (α) is then expressed as

$$\frac{\alpha}{1-\alpha} = \frac{k_{sol}}{k_{des}} = \frac{\exp(-\Delta G_{sol}/RT)}{\exp(-\Delta G_{des}/RT)} = \exp\left(\frac{-\Delta G_{obs}}{RT}\right) \quad (8)$$

The parameter $\Delta G_{obs} = \Delta H_{obs} - T\Delta S_{obs}$ is the Gibbs energy of the transition state between molecules in the gas phase and molecules solvated in the liquid phase. The functional form of ΔG_{obs} depends on the theoretical formulation of the uptake process. Therefore, the parameter ΔG_{obs} serves as a bridge between experiment and theory. Uptake studies on water surfaces led to the formulation of a nucleation critical cluster model for mass accommodation that successfully explained several features noted in our earlier uptake studies on aqueous surfaces including the observation that a plot of ΔH_{obs} versus ΔS_{obs} for all the species studied exhibits a near straight-line relationship.[7,8] As described in the preceding paper, the nucleation model for mass accommodation seems to apply likewise to the octanol surface for the organic gas-phase species discussed there.

The values for ΔH_{obs} and ΔS_{obs} can be obtained from the experimental results by plotting the natural log of $\alpha/(1-\alpha)$ as a function of $1/T$. The slope of such a plot is $-\Delta H_{obs}/R$ and the intercept is $\Delta S_{obs}/R$. The solid lines in Figure 3 are plots of eq 8 with best fit values for HCl of $\Delta H_{obs} = -(8.6 \pm 2.6)$ kcal mol^{-1} and $\Delta S_{obs} = -(41.3 \pm 9.7)$ cal mol^{-1} K^{-1} and for acetic acid $\Delta H_{obs} = -(8.1 \pm 1.4)$ kcal mol^{-1} and $\Delta S_{obs} = -(31.5 \pm 5.2)$ cal mol^{-1} K^{-1}.

Within the experimental accuracy, the mass accommodation coefficients of HBr and HI on octanol are 1. In fact, the formulation in eq 8 precludes the value of α to be exactly 1. ($\alpha = 1$ implies that $k_{sol}/k_{des} = \infty$.) Therefore, in the context of eq 8, the α-value for HBr and HI is understood to be close to, but not equal to, 1. For example, a value of $\alpha > 0.99$ implies $k_{sol}/k_{des} > 99$ and $-\Delta G_{obs}/RT > 4.6$. Since the mass accommodation coefficient of HBr is independent of temperature within the precision of the measurements, individual values for ΔH_{obs} and ΔS_{obs} cannot be determined in this case.

The larger value of α for HBr and HI on octanol indicates (via eq 8) that the ratio of k_{sol}/k_{des} is larger for HBr than that for HCl. In terms of the nucleation model this implies that HBr and HI interact more strongly with the octanol surface molecules than does HCl. A related observation was made by Ringeisen et al.[10] in experiments studying the collisions of HCl and HBr with liquid glycerol. Nearly all HBr molecules, thermalized at the glycerol surface, enter the bulk liquid, whereas a significant fraction (about 0.5) of the thermalized HCl departs the surface without entering into the bulk liquid. The stronger interaction of HI and HBr with octanol can perhaps be understood in terms of the polarizability and acidity of the hydrogen halides (HX) as was suggested by Ringeisen et al.[10]

The interactions of HX with octanol are expected to proceed via the following steps designated as **I**, **II**, and **III**:[11,12]

$$C_8H_{17}OH + HX \rightleftharpoons C_8H_{17}OH\text{--}HX\ (\mathbf{I}) \rightleftharpoons C_8H_{17}OH_2^+\ X^-\ (\mathbf{II}) \rightleftharpoons C_8H_{17}OH_2^+\ X^-\ (\mathbf{III}) \quad \text{(R-1)}$$

We expect that the entry of the HX molecules into liquid octanol is governed by the formation of the ionic complex **II**. The formation of this complex involves the scission of the X−H σ bond. The ease of this scission in turn depends on the polarizability (and consequently acidity) of the HX molecules.[11] The polarizability and acidity of the hydrogen halides increase in the order HCl < HBr < HI. The polarizabilities for the three molecules are 2.63, 3.61, and 5.44 Å^3, respectively.[13] The dissociation constants of HCl, HBr, and HI in water at 298 K are 1.2×10^8, 2.2×10^{10}, and 5.0×10^{10}, respectively.[14] Clearly, the mass accommodation coefficients for the HX molecules are in accord with these trends.

Acetic acid is a weaker acid than HCl ($K_a = 1.6 \times 10^{-5}$ and 1.2×10^8, respectively), yet its mass accommodation coefficient is about a factor of 20 higher. Clearly, the interaction of acetic acid with octanol is not governed by the acid properties of the molecule. In fact the interaction of acetic acid with octanol is similar to that of the organic gases described in the preceding article. This can be deduced from two observations. First, as is evident in Figure 10 of the preceding article, the ΔH_{obs} and ΔS_{obs} values for acetic acid fall on the same straight line as those for the organic gases. Second, as is the case for the organic gases, α for acetic acid is likewise unaffected by relative humidity. Whereas α for the HX gas-phase species exhibits the already noted dramatic relative humidity dependence.

In terms of the nucleation model of mass accommodation, the formation of the critical cluster leading to the uptake of the organic gases by octanol is expected to occur via the attractive interactions between the organic trace molecule and the hydrophobic part of octanol. The uptake of acetic acid is likewise likely to proceed via the mutual attraction of the hydrophobic parts of the two species (that is acetic acid and octanol).

Mass Accommodation as a Function of Relative Humidity. The behavior of the mass accommodation coefficient for the HX molecules as a function of relative humidity, displayed in

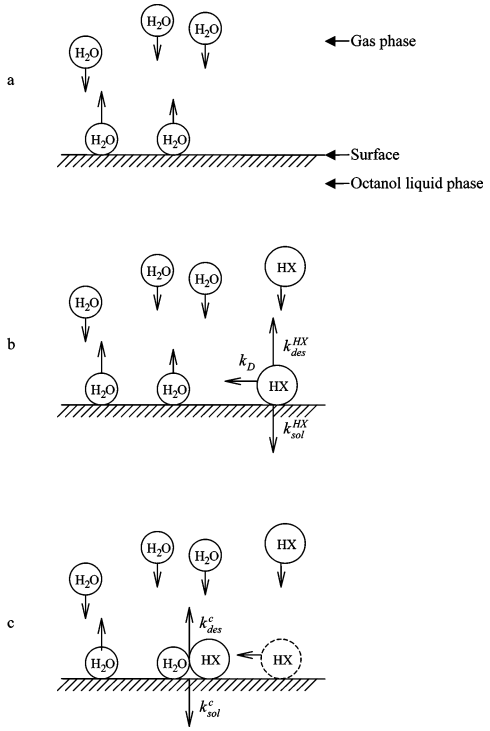

Figure 7. Representation of the kinetic model describing the uptake of the HX gas-phase acids in the presence of water vapor.

Figures 5 and 6, is certainly unexpected. Even at a low relative humidity of 50%, seemingly the uptake of every HX molecule that strikes the octanol surface is governed by water. On the other hand, the measured uptake of organic gases and acetic acid is unaffected by humidity.

At first glance it seems as if, at these low humidities, the entire octanol surface is covered by water molecules. Yet we know that this cannot be the case. Only a small fraction of a relatively hydrophobic surface, such as octanol, is expected to be occupied by water. As will be shown, even at 100% R.H. the water coverage on the octanol surface is only about 10%. (At this point the bulk mole fraction of water is about 0.2.) How then is one to account for the large effect of water vapor on an essentially hydrophobic octanol surface? Clearly the simple two-step process described by eq 9 of the preceding article[1] cannot explain the results.

Langmuir−Hinshelwood Model for Uptake of HX(g). The Langmuir−Hinshelwood mechanism has been used previously to elucidate heterogeneous processes in the atmosphere. For example, Ammann et al.[15] derived an expression via the Langmuir−Hinshelwood mechanism for the study of surface reaction on gas uptake by atmospheric particles. Remorov et al.[16] combined Eley−Rideal and Langmuir−Hinshelwood mechanisms to explain the experimental results of HO_2 uptake on solid NaCl. Here we utilize a Langmuir−Hinshelwood type kinetic model to describe the uptake of the HX gas-phase acids as a function of relative humidity. Quantitative values for the parameters characterizing the model are not available. Therefore, a rigorous test of the model is not feasible. However, by fitting the experimental data to the model, it will be possible to determine whether the values for the model parameters are physically reasonable. The model is represented schematically in Figure 7.

We begin by assuming that in the presence of gas-phase water, the octanol surface is in dynamic equilibrium with the water vapor (Figure 7a). In other words, when in equilibrium with water vapor, there is a population of water molecules (density n_s^w cm^{-2}) bound to the octanol surface. An HX molecule that lands on the octanol surface (and thermally accommodates to it) now may take three pathways. As before (that is in the absence of water), it may (1) desorb from the surface (rate constant k_{des}^{HX}), (2) enter into the bulk liquid (rate constant k_{sol}^{HX}), or (3) in the presence of surface-bound water molecules, it may encounter a surface water molecule and form a new HX−H_2O surface complex (rate of complex formation $n_s^w k_D$) (see Figure 7b). Here k_D is the surface diffusion controlled reaction rate constant. We have no information about the proposed HX−H_2O surface complex. Experimental[17] and theoretical[18,19] studies indicate that more than one water molecule is required for complete ionization of HX. The complex as we envision it involves initially only one water molecule. The surface HX is certainly not fully ionized. Subsequent association with additional water and/or octanol molecules may result in HX ionization once entry into the bulk liquid is initiated. The HX−H_2O surface complex is governed by its own desorption (rate constant k_{des}^c) and solvation (rate constant k_{sol}^c) kinetics (Figure 7c). The model is represented in eq 9.

$$\begin{array}{ccccc} n_g^{HX} & \underset{k_{des}^{HX}}{\overset{k_{ads}^{HX}}{\rightleftharpoons}} & n_s^{HX} & \xrightarrow{k_{sol}^{HX}} & n_l^{HX} \\ & & \downarrow n_s^w k_D & & \\ & & n_s^c & \xrightarrow{k_{sol}^c} & n_l^c \\ & & k_{des}^c \text{ (}\leftarrow\text{)} & & \end{array} \tag{9}$$

The representation shown in eq 9 makes it evident that if the rate $n_s^w k_D$ is sufficiently large, all the HX molecules that land on the octanol surface are converted into a HX−H_2O complex and the uptake is governed entirely by the surface kinetics of the complex. The rate equations for the process are

$$\frac{dn_s^{HX}}{dt} = \frac{n_g^{HX}\bar{c}}{4} - n_s^{HX} k_{sol}^{HX} - n_s^{HX} k_{des}^{HX} - n_s^{HX} n_s^w k_D \tag{10}$$

$$\frac{dn_s^c}{dt} = -n_s^c k_{sol}^c + n_s^{HX} n_s^w k_D - n_s^c k_{des}^c \tag{11}$$

$$\frac{\alpha_T n_g^{HX}\bar{c}}{4} = n_s^c k_{sol}^c + n_s^{HX} k_{sol}^{HX} \tag{12}$$

Here $\bar{c}$ is the average thermal speed and α_T is the overall mass accommodation coefficient for the species HX. Under steady-state conditions, eqs 10 and 11 yield

$$\frac{n_g^{HX}\bar{c}}{4} = n_s^{HX}(k_{sol}^{HX} + k_{des}^{HX} + n_s^w k_D) \tag{13}$$

and

$$n_s^c = \frac{n_s^{HX} n_s^w k_D}{k_{sol}^c + k_{des}^c} \tag{14}$$

Combining eqs 12−14, we obtain

$$\alpha_T = \frac{n_s^w k_D k_{sol}^c}{(k_{sol}^c + k_{des}^c)(k_{sol}^{HX} + k_{des}^{HX} + n_s^w k_D)} + \frac{k_{sol}^{HX}}{(k_{sol}^{HX} + k_{des}^{HX} + n_s^w k_D)} \quad (15)$$

We define the mass accommodation coefficient for the HX−H_2O surface complex as $\alpha_c = k_{sol}^c/(k_{sol}^c + k_{des}^c)$. Equation 15 then simplifies to

$$\alpha_T = \frac{\alpha_c n_s^w k_D + k_{sol}^{HX}}{k_{sol}^{HX} + k_{des}^{HX} + n_s^w k_D} \quad (16)$$

For convenience we repeat the definitions used in the above equations. α_T is the overall mass accommodation coefficient for HX (X = Cl, Br, I); α_c is the mass accommodation coefficient of the surface complex HX-H_2O; n_s^w is the surface concentration of water (cm^{-2}); k_{sol}^{HX} is the solvation rate constant of HX (s^{-1}); k_{des}^{HX} is the HX desorption rate (s^{-1}); and k_D is the second-order HX−H_2O surface reaction rate ($cm^2\ s^{-1}$);

In the absence of water vapor, the mass accommodation coefficient of HCl on octanol is very small ($\alpha < 0.01$ at 273 K), implying that the ratio ($k_{sol}^{HCl}/k_{des}^{HCl}$) is negligible compared to the other terms in eq 16. Therefore, for HCl eq 16 simplifies to

$$\alpha_T = \frac{\alpha_c n_s^w (k_D^{HCl}/k_{des}^{HCl})}{1 + n_s^w (k_D^{HCl}/k_{des}^{HCl})} \quad (17)$$

On the other hand, in the absence of water vapor, the mass accommodation coefficient of HBr is close to unity, implying $k_{sol}^{HBr} \gg k_{des}^{HBr}$. Therefore, for HBr eq 16 simplifies to

$$\alpha_T = \frac{1 + \alpha_c n_s^w (k_D^{HBr}/k_{sol}^{HBr})}{1 + n_s^w (k_D^{HBr}/k_{sol}^{HBr})} \quad (18)$$

α_c in eqs 17 and 18 is the mass accommodation coefficient at high R.H. (large n_s^w).

The measured mass accommodation coefficient α_T is a function of relative humidity and droplet temperature. Our aim is to globally fit, via eqs 17 and 18, the measured mass accommodation coefficients in Figure 5a,b at the three temperatures studied. The parameter α_c in eqs 17 and 18 is obtained from the measured α at high relative humidity. As will be shown, the surface density (n_s^w) of water molecules can be estimated via the equilibrium condition. This leaves one unknown ratio of rates in each equation to be obtained by fitting of the equation to the experimental data in the figures. The unknown is (k_D^{HCl}/k_{des}^{HCl}) in eq 17 and (k_D^{HBr}/k_{sol}^{HBr}) in eq 18.

We expect each of the rate coefficients in the ratios to have an Arrhenius type dependence on temperature, therefore the ratio (k_D^{HCl}/k_{des}^{HCl}) in eq 17 can be expressed as

$$\frac{k_D^{HCl}}{k_{des}^{HCl}} = C_{HCl} \exp(\Delta E_{HCl}/RT) \quad (19)$$

Similarly (k_D^{HBr}/k_{sol}^{HBr}) in eq 18 can be expressed as

$$\frac{k_D^{HBr}}{k_{sol}^{HBr}} = C_{HBr} \exp(\Delta E_{HBr}/RT) \quad (20)$$

Here T is the liquid temperature, and C_{HCl} and C_{HBr} are the preexponential constants. Because the ΔE term in each equation is the difference between the energy dependence of two rate constants, ΔE_{HCl} and ΔE_{HBr} can be either positive or negative. Note that the ratios in eqs 19 and 20 are in centimeters squared.

Surface Density of Water. The surface density (n_s^w) of water molecules is obtained via the equilibrium condition

$$n_s^w\, k_{des}^w = n_g^w \frac{\bar{c}}{4} \quad (21)$$

Here k_{des}^w (s^{-1}) is the desorption rate constant of water molecules from the liquid octanol surface and n_g^w is the density of gas-phase water molecules. (n_g^w is related to the partial pressure of water vapor (P_w) via the ideal gas law. The partial pressure of water over octanol−water solutions is derived in Appendix 1 of the preceding paper.[1]) The rate constant k_{des}^w is assumed to be of the form[20]

$$k_{des}^w = 10^{13} \exp(-\Delta E_{des}^w/RT) \quad (22)$$

where ΔE_{des}^w is the desorption energy of water molecules from the liquid octanol surface and the preexponential 10^{13} s^{-1} is the magnitude of typical molecular vibrational frequencies.

The value of ΔE_{des}^w is not known. However, it can be estimated from the solvation enthalpy (ΔH_{sol}^w) of water in liquid octanol that was measured to be −40 kJ/mol by Berti et al.[21] Adamson and Gast[20] suggested that the surface energy E_s^w of a molecule with respect to the bulk is about one-fourth of the solvation energy. Therefore, it follows that $\Delta E_{des}^w \cong -(\Delta H_{sol}^w - E_s^w) = 0.75(-\Delta H_{sol}^w) = 30$ kJ/mol. With this value of ΔE_{des}^w, eq 22 yields $k_{des}^w = 1.1 \times 10^7$, 1.8×10^7, and 2.9×10^7 s^{-1} for 263, 273, and 283 K, respectively. From eq 21 we obtain n_s^w (cm^{-2}) that can be expressed as a function of water vapor pressure as

$$n_s^w = AP_w \quad (23)$$

Here A is in cm^{-2} $Torr^{-1}$ and at the three temperatures studied, 263, 273, and 283 K, its value is 4.6×10^{13}, 2.8×10^{13}, and 1.7×10^{13}, respectively.

With the values of n_s^w given by eq 23, the global fitting of α_T for HCl via eq 17 yields (with RT in kJ/mol)

$$\frac{k_D^{HCl}}{k_{des}^{HCl}} = (2.07 \times 10^{-12}) \exp(-10.1/RT)\ cm^2$$

and for the HBr data eq 18 yields

$$\frac{k_D^{HBr}}{k_{sol}^{HBr}} = (5.00 \times 10^{-16}) \exp(13.8/RT)\ cm^2$$

The single temperature study for HI at $T = 273$ K yields

$$\frac{k_D^{HI}}{k_{sol}^{HI}} = 1.43 \times 10^{-13}\ cm^2$$

The rate constant ratios at the experimental temperatures obtained from the model fitting of the data are listed in Table 4.

We will now examine whether the magnitudes of the rate constant ratios in Table 4 are reasonable.

TABLE 4: Fitting Parameters for HX Uptake by 1-Octanol

	temp (K)	k_D^{HX}/k_{des}^{HX} (cm^2)	k_D^{HX}/k_{sol}^{HX} (cm^2)
HCl	263	2.04×10^{-14}	
	273	2.42×10^{-14}	
	283	2.83×10^{-14}	
HBr	263		2.75×10^{-13}
	273		2.18×10^{-13}
	283		1.76×10^{-13}
HI	273		1.43×10^{-13}

TABLE 5: Estimated Values of k_{des}^{HCl} and k_D^{HCl} for HCl

	temp (K)	k_{des}^{HCl} (s^{-1})	k_D^{HCl} ($cm^2\ s^{-1}$)
HCl	263	7.99×10^6	1.63×10^{-7}
	273	1.34×10^7	3.24×10^{-7}
	283	2.15×10^7	6.08×10^{-7}

TABLE 6: Estimated Maximum Values of k_{sol}^{HBr} and $(k_D)_{max}$ for HBr

	temp (K)	k_{sol}^{HBr} (s^{-1})	$(k_D)_{max}$ ($cm^2\ s^{-1}$)
HBr	263	1.09×10^8	2.99×10^{-5}
	273	1.56×10^8	3.40×10^{-5}
	283	2.18×10^8	3.83×10^{-5}

Evaluation of Modeling Results. None of the rate constants in Table 4 are known individually. However, a reasonable estimate can be obtained for k_{des}^{HCl} and the maximum value for k_D can also be obtained.

To estimate k_{des}^{HCl} for HCl, we assume that the rate constant is of the form $k_{des}^{HCl} = 10^{13} \exp(-\Delta E_{des}^{HCl}/RT)$. Here ΔE_{des}^{HCl} is the desorption energy of HCl from the liquid octanol surface. ΔE_{des}^{HCl} for HCl has not been measured. However, the solvation energy of HBr (ΔH_{sol}^{HBr}) in liquid octanol was measured to be about -41 kJ/mol.[22] To estimate k_{des}^{HCl} we will assume that the same value holds for HCl. Further, as before we will assume that $\Delta E_{des}^{HCl} = -0.75 \times \Delta H_{sol}^{HCl} = 30.7$ kJ/mol. The calculated values of k_{des}^{HCl} and k_D^{HCl} obtained from the ratios (k_D^{HCl}/k_{des}^{HCl}) for HCl are listed in Table 5.

The analysis of the HBr data is somewhat less firm. The value of k_{sol}^{HBr} cannot be readily evaluated. However, the maximum value of k_D ($(k_D)_{max}$) can be obtained from the work of Allen and Seebauer[23] in terms of surface diffusion coefficient D_s as $(k_D)_{max} = 4D_s$. The parameter D_s can be expressed in terms of the frequency factor A, diffusion jump distance λ, and the surface diffusion activation energy E_s as $D_s = {}^1/_4 A\lambda^2 \exp(-E_s/RT)$.[20] To estimate D_s we will use typical order of magnitude values of $A = 10^{13}\ s^{-1}$ and $\lambda = 10^{-8}$ cm. The surface diffusion activation energy is usually taken to be about one-fourth of the desorption energy[20] (i.e. $E_s = 0.25\Delta E_{des} = 7.67$ kJ/mol for HX). The maximum estimated value of k_D and the corresponding maximum value of k_{sol}^{HBr} for HBr are listed in Table 6.

While the rate constant values in Tables 5 and 6 certainly cannot be considered as firm determinations, their magnitudes seem physically reasonable. Specifically we note that k_D^{HCl} is smaller than the limit set by the calculated value of $(k_D)_{max}$ as it must be. The magnitudes of the other rate constants likewise are in acceptable ranges. We also note that k_D^{HCl} at $10^{-7} cm^2\ s^{-1}$, while smaller than $(k_D)_{max}$, is considerably larger than the surface reaction rate coefficients for O_3 ($k_s = 10^{-17}\ cm^2\ s^{-1}$) obtained by Amman et al.[15] This large difference is perhaps explained by the nature of the interactions. The surface reactions described by Amman et al. are chemical reactions involving formation of new chemical bonds. However, the formation of a $HX-H_2O$ complex in our experiment is expected to involve polarization of species rather than bond breakage. The process is therefore expected to be more facile, not hindered by activation energy. In the absence of steric hindrance the complex formation rate could be as high as the surface diffusion limited rate.

We suggest that the Langmuir−Hinshelwood kinetic model provides a reasonable explanation for the observed uptake of the HX gas-phase acids as a function of relative humidity. Further work is in progress to test the model described in this article.

Finally, we would like to comment briefly on the connection between the Langmuir−Hinshelwood model calculations and the nucleation critical cluster model of mass accommodation. In modeling the HX uptake by octanol via eq 9 as a function of relative humidity, in the region where α is changing with water vapor density, the data are well fit by a linear dependence on the density of water molecules. That is, in the rate eqs 10 and 11, the surface water density (n_s^w) is taken to the power 1. Consequently the simplest assumption is that once an $HX-H_2O$ complex is formed, further aggregation of water molecules to the complex does not aid uptake by octanol. In other words, the formation of a critical cluster consisting of $HX-H_2O$ + octanol molecules now proceeds independently of additional water molecules that may associate to the cluster. From the perspective of the nucleation model of uptake, the one water molecule attached to HX enhances the formation rate of critical clusters incorporating HCl and decreases the corresponding process for HBr and HI. If the uptake of the HX species proceeds via the ionizing sequence shown in eq R-1, then one concludes that a water molecule complexed to HX(g) enhances ionization for HCl and hinders the process for HBr and HI. At this point the reason is not evident.

All atmospheric chemistry proceeds in the presence of water vapor. This work demonstrates the dramatic effect of water vapor on the uptake of HX(g) by an organic substance such as octanol. The possible importance of such a phenomenon in the atmosphere needs to be further explored.

Acknowledgment. We thank Prof. Heather C. Allen for helpful discussions. Funding for this work was provided by the National Science Foundation Grant Nos. ATM-0212464 and CH-0089147, by the Department of Energy Grant No. DE-FG02-98ER62581, and by the US-Israel Binational Science Foundation Grant No. 1999134.

References and Notes

(1) Zhang, H. Z.; Li, Y. Q.; Xia, J. R.; Davidovits, P.; Williams, L. R.; Jayne, J. T.; Kolb, C. E.; Worsnop, D. R. *J. Phys. Chem. A* **2003**, *107*, 6388.

(2) Worsnop, D. R.; Shi, Q.; Jayne, J. T.; Kolb, C. E.; Swartz, E.; Davidovits, P. *J. Aerosol Sci.* **2001**, *32*, 877.

(3) Shi, Q.; Davidovits, P.; Jayne, J. T.; Worsnop, D. R.; Kolb, C. E. *J. Phys. Chem. A* **1999**, *103*, 8812.

(4) Robinson, G. N.; Worsnop, D. R.; Jayne, J. T.; Kolb, C. E.; Swartz, E.; Davidovits, P. *J. Geophys. Res.* [*Atmospheres*] **1998**, *103*, 25371.

(5) Jayne, J. T.; Duan, S. X.; Davidovits, P.; Worsnop, D. R.; Zahniser, M. S.; Kolb, C. E. *J. Phys. Chem.* **1991**, *95*, 6329.

(6) Reid, R. C.; Prausnitz, J. M.; Poling, B. E. *The Properties of Gases and Liquids*; MacGraw Hill: New York, 1987.

(7) Davidovits, P.; Jayne, J. T.; Duan, S. X.; Worsnop, D. R.; Zahniser, M. S.; Kolb, C. E. *J. Phys. Chem.* **1991**, *95*, 6337.

(8) Nathanson, G. M.; Davidovits, P.; Worsnop, D. R.; Kolb, C. E. *J. Phys. Chem.* **1996**, *100*, 13007.

(9) Kolb, C. E.; Davidovits, P.; Worsnop, D. R.; Shi, Q.; Jayne, J. T. *Prog. Kinet. Mech.* **2002**, *27*, 1.

(10) Ringeisen, B. R.; Muenter, A. H.; Nathanson, G. M. *J. Phys. Chem. B* **2002**, *106*, 4988.

(11) Janz, G. J.; Danyluk, S. S. *Chem. Rev.* **1960**, *60*, 209.
(12) Ahmed, W.; Gerrard, W.; Maladkar, V. K. *J. Appl. Chem.* **1970**, *20*, 109.
(13) Lide, D. R. *CRC Handbook of Chemistry and Physics*, 73th ed.; CRC Press: Boca Raton, FL, 1992.
(14) Liptrot, G. F.; Thompson, J. J.; Walker, G. R. *Modern Physical Chemistry*; Bell and Hyman: London, UK, 1981.
(15) Ammann, M.; Poeschl, U.; Rudich, Y. *Phys. Chem. Chem. Phys.* **2003**, *5*, 351.
(16) Remorov, R. G.; Gershenzon, Y. M.; Molina, L. T.; Molina, M. J. *J. Phys. Chem. A* **2002**, *106*, 4558.
(17) Hurley, S. M.; Dermota, T. E.; Hydutsky, D. P.; Castleman, A. W., Jr. *Science* **2002**, *298*, 202.
(18) Conley, C.; Tao, F.-M. *Chem. Phys. Lett.* **1999**, *301*, 29.
(19) Chipot, C.; Gorb, L. G.; Rivail, J. L. *J. Phys. Chem.* **1994**, *98*, 1601.
(20) Adamson, A. W.; Gast, A. P., Eds. *Physical Chemistry of Surfaces*, 6th ed.; Wiley: New York, 1997.
(21) Berti, P.; Cabani, S.; Conti, G.; Mollica, V. *J. Chem. Soc., Faraday Transactions 1* **1986**, *82*, 2547.
(22) Fernandes, J. B. *J. Chem. Eng. Data* **1972**, *17*, 377.
(23) Allen, C. E.; Seebauer, E. G. *J. Chem. Phys.* **1996**, *104*, 2557.
(24) Van Doren, J. M.; Watson, L. R.; Davidovits, P.; Worsnop, D. R.; Zahniser, M. S.; Kolb, C. E. *J. Phys. Chem.* **1990**, *94*, 3265.
(25) Zhang, H. Z. Uptake of atmospherically relevant trace gases on organic liquids. Doctoral Thesis, Boston College, 2003.